C-3

EXACT IMAGE THEORY FOR FIELD CALCULATION IN LAYERED BIOLOGICAL MEDIUM

Esko Alanen, Ismo V. Lindell

Electromagnetics laboratory,
Helsinki University of Technology, Finland

Summary

A method based on the exact image theory to calculate the near field distribution of a horn antenna in direct contact with the skin is introduced. Being exact, the method is not restricted by parameter values and can be applied in optimization of horn aperture function to produce focus fields in the human body. The method observes the effect of the skin layer and can be applied for an arbitrary aperture function. The optimization is demonstrated with few examples.

Introduction

During the past decade a considerable effort has been aimed at the problem of irradiative treatment of living organism using the microwave range of frequency. The present contribution is a theoretical wievpoint on the subject, we beleave that combining the practical and theoretical knowledge a significant improvement of the applicators could be achieved. Microwave thermography resiprocically shares the same difficulties, which are the poor focusing of the radiation energy because the distances are of the order of wavelength, and serious problems in field calculation at the near field range.

In this study we concider a rectangular horn antenna in direct contact with the skin in either active or passive use, During some practical research in Helsinki University of Technology the following questions have arised: should the aperture size be increased or decreased to get a greater concentration of the fields in the near field range, and, is there an aperture funtion, as has been proposed e.g. in (1), which would offer better resolution at a certain depth than the ordinary ones. The aim of this study is to derive exact field equations for arbitrary aperture functions and then by varying the phase of the function demonstate the near field focusing.

The present approach applies the exact image theory in solving a three-layer problem shown in Fig. 1d. The real conficuration is shown in Fig. 1a, in Fig. 1b the Huygens' sources are placed at the aperture plane, the electric sources vanishes because of the ideal conductor in Fig.1c, which directly leads to the symmetric three-layer problem of Fig. 1d.

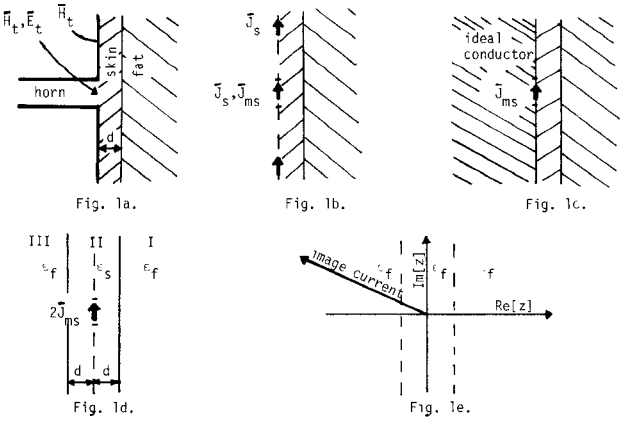

Fig. 1a. Fig. 1b. Fig. 1c. Fig. 1d. Fig. 1e.

Fig. 1a-e. The construction of the symmetric three layer problem.

The exact image theory was introduced by the authors recently (2-4). The basic idea is simple: the half-space below the primary point source is replaced by an image source which together with the original source gives the exact field, see Fig. 2. The image is a continuous source distribution along the z-axis, the z-coordinate of the image is extended into complex plane for the best convergence of the image fuction. In real space the function would be divergent and thus useless. Because the image function is situated in complex space, the Green function is exponentially decaying and the field integration is furher improved.

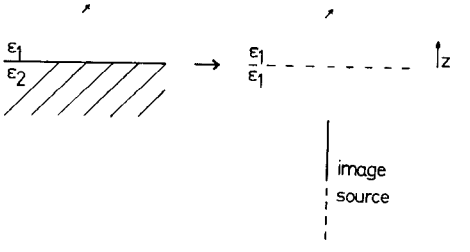

Fig. 2. The exact image solution for a point-excitation above a homogeneous half-space.

0149-645X/85/0000-0078 $01.00 © 1985 IEEE

For vertical sources the image consists of a vertical component, only. For horizontal sources the image is composed of both a vertical and a horizontal component, for a point source excitation the vertical image is multiplyed by the derivative of the delta-function of a horizontal coordinate. The appearance of the image of a horizontal source is illustrated in Fig. 3, the location on complex z-plane is also shown. The exact image corresponding to a general three-dimensional source was given in (4).

Up to the present the theory was applied only to two-layer Sommerfeld problems (5-6).

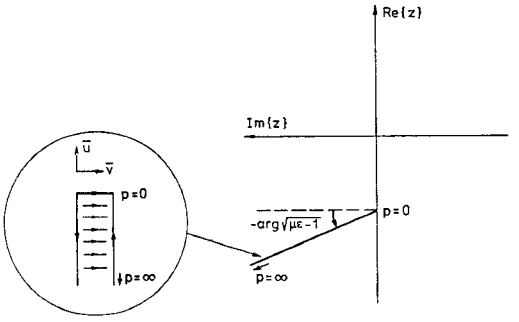

Fig. 3. The image of a horizontal dipole.

The image currents

The expression for the image function can be derived from the Fourier transformed problem. The field is not directly inverse transformed but expressed as a field of a line current distribution involving the inverse Laplace transform of the Fourier domain transmission coefficient. The inverse is best convergent on a particular path on the complex plane, which determines the location of the image current in complex space.

The formulation presented in (4) can be extended for the present three-layer case in Fig. 1d. The following equations determine the image for a horizontal point source, for a two-dimensional aperture function the solution can be integrated from this.

The Maxwell equations are expressed in terms of the tranverse electric and magnetic fields $\bar{e}$ and $\bar{h}$ in Fourier domain. Requiring the continuity of the transverse fields the solution $\bar{e}_1$ in the region I of Fig. 1d can be expressed for the primary source $\bar{J}_m = I_m L\ \delta(x)\delta(y)\delta(z)\bar{u}_x$ as follows:

$$\bar{e}_1 = -0.5\ \bar{b}\cdot\bar{\bar{T}}_k\ e^{uz} \tag{1}$$

$$\bar{b} = I_m L\ \bar{u}_y \tag{2}$$

where

$$\bar{\bar{T}}_k = F(u)\ \bar{\bar{I}}_t + G(u)\ \frac{\bar{K}\bar{K}}{k^2} \tag{3}$$

$$F(u) = -e^{-d(u_2-u)}\ \frac{1 + R_{TE}}{1 + e^{-2u_2 d}\ R_{TE}} \tag{4}$$

$$G(u) = -e^{-d(u_2-u)}\ \left\{\frac{1 + R_{TM}}{1 + e^{-2u_2 d}\ R_{TM}} - \frac{1 + R_{TE}}{1 + e^{-2u_2 d}\ R_{TE}}\right\} \frac{k^2}{K^2} \tag{5}$$

In (3)-(5)

$$R_{TE} = \frac{u_2 - u}{u_2 + u}$$

$$R_{TM} = \frac{\varepsilon u - u_2}{\varepsilon u + u_2}$$

$$u = \sqrt{K^2 - \varepsilon_1 k^2}\ , \quad \varepsilon_1 = \varepsilon_f/\varepsilon_o\ , \quad \varepsilon_2 = \varepsilon_s/\varepsilon_o$$

$$u_2 = \sqrt{u^2 - \Delta\varepsilon k^2}\ , \quad \Delta\varepsilon = \varepsilon_2 - \varepsilon_1$$

$$\mathrm{Re}(u, u_2) > 0\ , \quad \varepsilon = \varepsilon_2/\varepsilon_1$$

$$k = \omega\sqrt{\varepsilon_o \mu_o}\ .$$

$\bar{K}$ is the two dimensional Fourier transform parameter.

The image source is constructed from a horizontal magnetic current and vertical electric current distribution. The latter could as well be a magnetic current distribution with a different magnitude function. Let the currents be following:

$$\bar{J}_m(z') = -I_m L\ \delta(\bar{\rho})\ \bar{u}_x \sum_i f_i(t_i)\ , \quad z' = -t_i \tag{6}$$

$$\bar{J}(z') = -j\ I_m L\ \frac{\varepsilon_1}{\mu_o}\ \frac{1}{k}\ \frac{\partial}{\partial y}\ \delta(\bar{\rho})\ \bar{u}_z \sum_i g_i(t_i),\ z' = -t_i \tag{7}$$

where each contour of t_i is arbitrary on complex plane.

It can be shown that if the magnitude functions f(t) and g(t) satisfy the Laplace transforms

$$F(u) = \sum_i \int f_i(t_i)\, e^{-ut_i}\, dt_i \qquad (8)$$

$$G(u) = \sum_i \int g_i(t_i)\, e^{-ut_i}\, dt_i \qquad (9)$$

the sources (6) and (7) are correct images.

f(t) and g(t) can be solved from (8) and (9) with suprising simplicity, because the transmission functions F(u) and G(u) are single-valued; the double-valued function $u_2=u_2(u)$ does not introduce branch points in F(u) and G(u) because they are invariant for the change of sign $u_2 \rightarrow -u_2$, which can be easily checked.

Thus the only singularities of F(u) and G(u) are the poles, infinite in number. Further on, the functions are bounded when $|u|\rightarrow\infty$. If all the poles are extracted from F(u) and G(u), according to Liouville's theorem the remaining functions must be constants. Therefore the following expressions can be written:

$$F(u) = f_0 + \sum_{i=1}^{\infty} \frac{f_i}{u-u_{pi}} \qquad (10)$$

$$G(u) = g_0 + \sum_{i=1}^{\infty} \frac{g_i}{u-u'_{pi}} \qquad (11)$$

From (10) and (11) can be deduced that f(t) and g(t) are sums of exponential functions. Further, it can be shown that all the exponential functions in f(t) and all but one in g(t) are decaying so rapidly that they can be replaced by a δ-function which can be surerposed. Finally, f(t) and g(t) are expressed as follows:

$$\sum_i f_i(t_i) \cong F(0)\ \delta(t) \qquad (12)$$

$$\sum_i g_i(t_i) \cong \left(G(0) + \frac{g_1}{u'_{p1}}\right) \delta(t) + g_1 e^{u'_{p1} t_1}, \qquad (13)$$

where the best contour of t_1 is the negative imaginary axis. With the dielectric factors of fat and skin and the skin thickness

$\varepsilon_f/\varepsilon_o = 5.5 - j0.85$, $\varepsilon_s/\varepsilon_o = 44 - j14$,

d = 1.5 mm,

the coefficients u'_{pi} and g_1 are

$u'_{p1} = (1.045 - j0.368)k$, $g_1 = (-0.297 + j0.103)k$.

Numerical demonstrations

The image sources for a point excitation (6) and (7) can be extended for a horn antenna with the aperture function

$$A(x,y) = \cos\left(\frac{\pi}{2}\frac{y}{a}\right) e^{jk(b_1|x| + b_2 x^2)}, \qquad (14)$$

size of the aperture a x b,

by integrating the solution in two dimensions. The cosine function in (14) corresponds to the TE_{10} mode of a rectangular waveguide.

The energy distribution at the depth of 3 cm in fat tissue was calculated with different phase parameters b_1, b_2. Special attention was paid on the reduction of the 3 dB focus extension in x-direction.

Similar calculations were carried out in y-direction. However, the reduction of the focus was weaker in these calculations.

Three different aperture sizes were considered and distinct optimum values for b_1 and b_2 were found. These are shown in table 1 with the 3 dB extensions in both x and y-directions. Also normalized maximum field strengths $|E(x=0, y=0)|$ are shown, and the corresponding values for constant phase apertures. The field strengths at the depth of 3 cm and with x=0...3 cm, y=0 can be seen in Fig. 4.

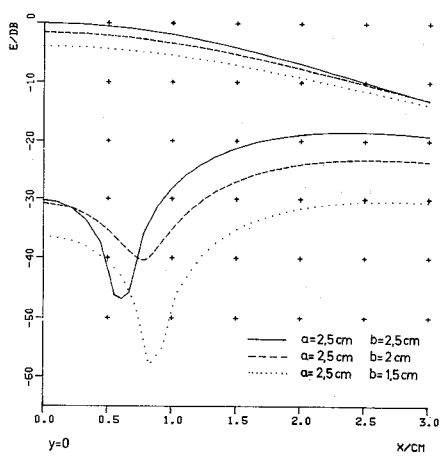

Fig. 4. The optimized curves (lower) and the constant phase curves (upper).

a/b (cm)	b_1/b_2	x_{3dB}	y_{3dB}	E_o
2.5/1.5	8/0.2	0.86	3.64	-36
2.5/2	6.1/0.1	0.84	3.02	-31
2.5/2.5	5.2/0	0.64	4.32	-30
2.5/1.5	0/0	2.92	3.60	-3.9
2.5/2	0/0	2.70	3.64	-1.6
2.5/2.5	0/0	2.54	3.68	0

Table 1. The optimum values of b_1/b_2. The minimum values of the focus extensions are squared separately.

The low values of the maximum field strengths E_o of the optimum points above may cause trouble in technical realization of the applicator. Therefore some results are shown in Fig. 5, where E_o is higher but the focal extension is larger.

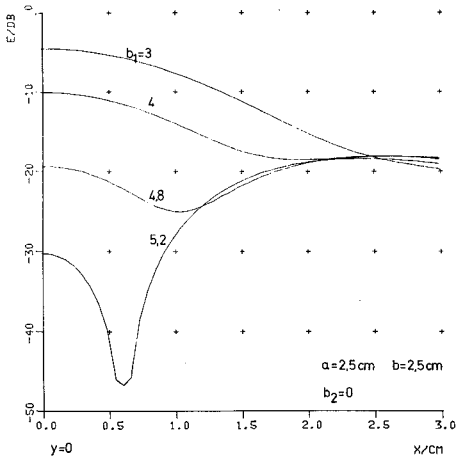

Fig. 5. Curves with higher E_o and larger focal extensions.

The numerical results above indicate that the maximum value of E_o is achieved very near the constant phase point $b_1=b_2=0$. The reason for this is the domination of the magnetic source (6) when the phase variation of the aperture is small. The phase of the electric field at the central axis arising from different points of this two-dimensional source is nearly constant, and thus the phase variation of the aperture function does not increase E_o. Therefore it is obvious that also the electric source (7) must be utilized in generating the hot spot. This requires the suppressing of the magnetic source by the phase variation.

Finally, the functions $x_{3dB}(b_1)$ and $E_o(b_1)$ with $b_2=0$, a=b=2.5 cm, are sketched in Fig. 6.

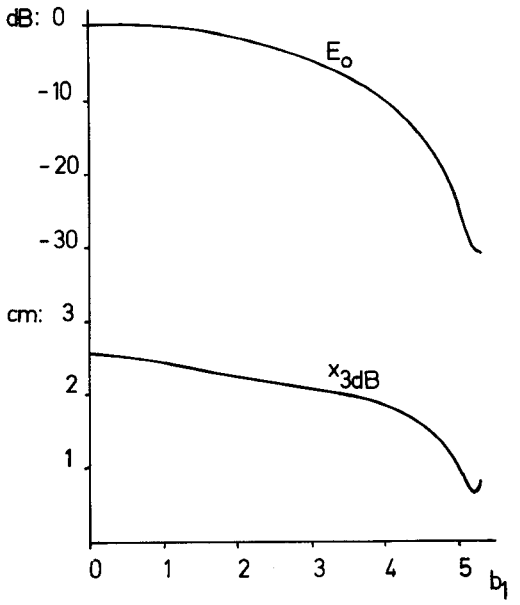

Fig. 6. The functions $E_o(b_1)$ and $x_{3dB}(b_1)$.

References

(1) P. S. Neelakantaswamy, K. K. Kupta, D. K. Banerjee, "A Gaussian-beam launcer for microwave exposure studies," IEEE Trans. Microwave Theory Tech., 25, pp. 426-428, (1977)

(2) I. V. Lindell, E. Alanen, "Exact image theory for the Sommerfeld half-space problem, Part I: Vertical magnetic dipole," IEEE Trans. Antennas Propagat., 32, pp. 126-133, (1984)

(3) - , " - , Part II: Vertical electric dipole," IEEE Trans. Antennas Propagat., 32, pp. 841-847, (1984)

(4) - , " - , Part III: General formulation," IEEE Trans. Antennas Propagat., 32, pp. 1927-1032, (1984)

(5) I. V. Lindell, E. Alanen, K. Mannersalo," Image method of antenna analysis in the presence of the ground," Journée Internationales de Nice sur les Antennes, Nice 13-15 novembre 1984, pp. 47-51

(6) E. Alanen, I. V. Lindell, "Impedance of vertical electric and magnetic dipole above a dissipative ground," Radio Science, 19, pp. 1469-1474, (1984)